TÜBİTAK

Turkish Journal of Botany

http://journals.tubitak.gov.tr/botany/

Research Article

Turk J Bot
(2013) 37: 1115-1124
© TÜBİTAK
doi:10.3906/bot-1211-47

Localization and distribution of nickel and other elements in in-vitro grown *Alyssum corsicum* exhibiting morphological changes in trichomes: initial insights into molecular mechanisms of nickel hyperaccumulation

Seniha Selcen BABAOĞLU AYDAŞ[1], Leyla AÇIK[1,*], Danika LEDUC[2], Nezaket ADIGÜZEL[1], Şeküre Şebnem ELLİALTIOĞLU[3], Zekiye SULUDERE[1], Yusuf Kağan KADIOĞLU[4]

[1]Department of Biology, Faculty of Science, Gazi University, Teknikokullar, Ankara, Turkey
[2]Department of Chemistry & Biochemistry, College of Science, California State University, East Bay, Hayward, California, USA
[3]Agricultural Faculty, Ankara University, Dışkapı, Ankara, Turkey
[4]Department of Geological Engineering, Faculty of Engineering, Ankara University, Tandoğan, Ankara, Turkey

Received: 22.11.2012 • **Accepted:** 21.07.2013 • **Published Online:** 30.10.2013 • **Printed:** 25.11.2013

Abstract: *Alyssum corsicum* Duby is a candidate plant used for phytomining and phytoremediation studies with its high Ni-accumulating ability of the aboveground tissues. Metal localization and concentration by hyperaccumulator plants and the physiological basis of these phenomena have been of great interest in recent years. *A. corsicum* seeds were grown at different concentrations of Ni in Murashige and Skoog medium. Multielement concentrations of the plant roots and shoots were determined by polarized energy dispersive X-ray fluorescence. Ni, Ca, Mg, and Fe localization and concentration at the upper and lower leaf surfaces were determined by scanning electron microscopy coupled with the energy-dispersive X-ray analysis technique (SEM-EDX). Results showed that Ni is accumulated more by the shoots than the roots of the plant and that Ni is concentrated mainly in the trichome and the stoma guard cells of the leaves. Trichome density on the leaves was reduced, and some morphological changes of the trichome structure were also observed with increasing Ni levels. Analysis of antioxidant enzyme activities in roots and shoots was performed. The total leaf proteins of the plant were examined by sodium dodecyl sulfate polyacrylamide gel electrophoresis, and differentially expressed genes were detected by specifically designed primers.

Key words: *Alyssum corsicum*, polarized energy dispersive X-ray fluorescence, antioxidant enzymes, differentially expressed genes

1. Introduction

Although heavy metals are toxic at high concentrations because of the damage they cause to plant metabolism, some metal-tolerant plants accumulate heavy metals within their aboveground tissues at high concentrations without any symptoms (Psaras et al., 2000; Pilon-Smits, 2005). Nickel hyperaccumulator plants are the largest group of metal hyperaccumulator plants with over 400 taxa, and the genus *Alyssum* L. (Brassicaceae) is the representative of this group with more than 50 nickel-hyperaccumulating species (Broadhurst et al., 2009). The accumulated Ni concentration reaches nearly 3% of the leaf dry biomass in many *Alyssum* species (Krämer et al., 1996; Altınözlü et al., 2012).

Serpentine soils are rich in heavy metals including nickel, cobalt, and chromium and are low in nutrients because they are derived from ultramafic rocks; therefore, a unique flora spreads out on such soil types (Prasad, 2005). Turkey is one of the major centers of hyperaccumulator plants as over half of the *Alyssum* species and over half of the hyperaccumulators are found in Turkey (Reeves and Adıgüzel, 2008). *Alyssum murale* Waldst. & Kit. and *A. corsicum* Duby are endemic to serpentine soils throughout Mediterranean Europe and are the species most often subjected to phytoremediation and phytomining studies because of their ability to grow in different types of soils (Brooks et al., 2000; Broadhurst et al., 2004). Plants hyperaccumulating heavy metals draw attention with the complex mechanisms they use to avoid the toxicity of heavy metals and where they accumulate such levels of heavy metals within the plant. Plants have a regulated system that consists of metal transport, chelation, transfer, and sequestration activities, all of which contribute to the uptake, distribution, and detoxification of metal ions (Clemens, 2001).

* Correspondence: leylaacik@gmail.com

X-ray fluorescence spectrometry (XRF) and similar methodologies for direct analysis of the metal content of plant samples have been applied to different species over the past few years. This technique allows the detection of specific elements by measuring their characteristic X-ray emission wavelength (WDXRF) or energy (EDXRF) (Margui et al., 2005). Scanning electron microscopy coupled with energy dispersive X-ray analysis techniques (SEM-EDX) is used in advance to determine the distribution of metals in plant tissues. Metal hyperaccumulation, especially nickel enrichment, is generally observed in the leaf tissue of the plants (Marmiroli et al., 2004).

Heavy metals may disturb the plant metabolism in multiple ways, causing a reduction of chlorophyll content, inhibiting plant growth and respiration, changing the ultrastructure of the cell organelles, and altering the activity and quantity of the key enzyme of various metabolic pathways. These effects may be closely related to the accumulation of heavy metals and the excessive production of reactive oxygen species (ROS) in plants, including superoxide radical (O2•−), hydroxyl radical (•OH) and hydrogen peroxide (H_2O_2) (Guo et al., 2007).

Ni can induce oxidative stress by disrupting the balance of formation and destruction of active oxygen species associated with normal cellular metabolism. Ni-induced deactivation of proteins, including antioxidant enzymes, and depletion of low-molecular-weight antioxidants are the possible mechanisms. Lipid peroxidation, which degrades membrane lipids and causes conformational changes in membrane proteins, has been observed in plants affected by Ni toxicity. Antioxidant enzymes such as superoxide dismutase (SOD), catalase (CAT), glutathione reductase (GR), and ascorbate peroxidase (APX) protect cells against oxygen radicals and peroxidation reactions (Boominathan and Doran, 2007; Öztürk Ürek and Tarhan, 2012).

The aims of this study were to determine the total amount of nickel accumulated by *A. corsicum*; to define the metal composition in the leaf, shoot, and root tissues; and to determine how the distribution of nickel in leaf tissues is related to the concentrations of the elements Mg, Ca, and Fe. Additionally, leaf protein patterns, antioxidant enzymes, and differential gene expression experiments were used to elucidate the molecular mechanisms involved in plant response to nickel treatment.

2. Materials and methods

2.1. Plant culture

Alyssum corsicum Duby seeds were collected by N Adıgüzel from serpentine soil in Tavşanlı, Kütahya (collection number: N. A. 3653). After surface sterilization, 16 seeds were sown per Magenta vessel containing Murashige and Skoog (MS) medium (Murashige and Skoog, 1962). Media included 0.0 mM, 0.01 mM, 0.04 mM, and 0.2 mM $NiCl_2.6H_2O$ in each experimental group. All equipment was decontaminated from metals with 10% HNO_3 solution overnight. Seed germination and plant growth took place in a growth chamber (Sanyo MLR- 315H, Japan) with 16 h of light (22 ± 1 °C, 50 ± 3% relative humidity) and 8 h of dark (19 ± 1 °C, 50 ± 3% relative humidity) (Abou Auda et al., 2002). After 2 months, plants were collected separately for SEM and PEDXRF analysis and rinsed thoroughly with deionized water.

2.2. PEDXRF analysis

2.2.1. Sample preparation for multielement analysis by PEDXRF

The samples were sun-dried and then ground into fine powder in an agate mortar. The samples were made to pass through a sieve of 200 µm and then pressed into thick pellets of 32 mm in diameter using wax as a binder. US Geological Survey standards (Geological Society) sediment standard GBW 7109 and plant material standards K04-BCR-60 (aquatic plant), K04-BCR-61 (aquatic moss), and K04-BCR-62 (oil-containing leaves) were pressed into pellets in a similar manner as the samples, and these were used for quality assurance (Timothy and Tour, 1989; Johnson et al., 1999).

2.2.2. PEDXRF measurements

Multielement concentration was determined using PEDXRF. The spectrometer used in this study was a Spectro XLAB 2000 PEDXRF spectrometer (Germany), which was equipped with a Rh anode X-ray tube and 0.5-mm Be side window. The spectrometer detector was Si (Li), cooled by liquid N_2, and had a resolution of <150 eV at Mn Kα, 5000 cps. Total analysis time for each additional element was 30 min. If the sample to be analyzed was excited with linear polarized X-ray radiation, only the fluorescence radiation excited in the measurement sample and, ideally, none of the primary radiation scattered by the sample reached a suitably positioned detector.

2.3. SEM-EDX analysis

The third leaves near the apical tips of stems were used for the SEM-EDX analysis. Whole fresh leaves were fixed for 24 h in 2.5% glutaraldehyde (pH 7.2, phosphate-buffered). Specimens were then rinsed 2 or more times with distilled water. This was followed by dehydration in a graded series of ethanol (from 70% to 100%). Leaves were then passed through amyl acetate. The sample was next dried at the critical point with CO_2 (Polaron, CPD 7501). They were mounted with double-sided tape on SEM stubs, coated with gold in a Polaron SC 502 Sputter Coater, and examined with a JEOL JSM 6060 (Japan) scanning electron microscope at 10–20 kV. The trichomes and stoma on the upper and lower surface of leaves were examined by SEM, and micrographs were taken digitally. The EDX spectra

analyses were performed with a JEOL JSM 6060 scanning electron microscope equipped with an IXRF-EDS 2000. SEM observations were achieved with 3 leaves from 3 different plants from both control and Ni-applied groups.

2.4. Protein extraction and gel electrophoresis

Protein extraction was performed according to the methods of Hajduch et al. (2001). A fresh leaf sample (0.1 g) was extracted with 100 µL of 0.2 M Tris-HCL buffer (pH 7.8) with chilled mortar and pestle. The homogenate was centrifuged at 18,500 × *g* at 4 °C for 5 min, and the supernatant was further centrifuged for 10 min. A 100-µL mixture of supernatant (78 µL) and blue juice (22 µL; 9% v/v 2-mercaptoethanol, 22.7% w/v sucrose, 4.5% w/v SDS, and 0.01% w/v bromophenol blue) was prepared, and the samples were boiled for 30 min before the electrophoresis on 15% polyacrylamide gel (5% stacking and 15% separation gel) at a constant current of 20 mA. Protein bands were visualized by staining the gels with Coomassie Brilliant Blue.

2.5. Enzyme activities

Enzyme extraction was achieved according to the method of Schickler et al. (1999). Fresh leaf and root samples were stored at –80 °C after harvesting and sampling for enzyme extraction. Fresh leaf and root samples were extracted in extraction buffer (50 mM phosphate buffer, pH 7.0, 1.0 mM EDTA, 0.05% (v/v) Triton X-100, 2% (w/v) polyvinylpolypyrrolidone, and 1 mM ascorbic acid) with Xiril Dispomix homogenizer (Germany) at 1000 rpm. After centrifuging at 16,500 × *g* for 5 min, the extracts were stored in aliquots at –80 °C. Total protein amount was determined with a Bradford assay (Bradford, 1976). CAT, GR, and AP activities were monitored with a Shimadzu UV1700 (Japan) spectrophotometer according to the method of Çakmak et al. (1994). A protein extract of 30 µg was used in enzyme activity measurements. The activity of ascorbate peroxidase was measured by monitoring the rate of ascorbate oxidation at 290 nm (E = 2.8 mM cm^{-1}). The reaction mixture contained 50 mM phosphate buffer (pH 7.6), 10 mM EDTA, 12 mM H_2O_2, and 0.25 mM L^{-1} ascorbic acid with enzyme extract. CAT activity was assayed in a reaction mixture containing 50 mM phosphate buffer (pH 7.6), 100 mM H_2O_2, and enzyme mixture. The decomposition of H_2O_2 was followed at 240 nm (E = 39.4 mM cm^{-1}). GR activity was measured in a reaction mixture containing phosphate buffer (pH 7.6), 0.5 mM oxidized glutathione, 0.12 mM NADPH, and enzyme aliquot following the decrease in absorbance at 340 nm due to NADPH oxidation (E = 6.2 mM cm^{-1}). Each measurement was carried out with 3 sequential dilutions in triplicate. The results were expressed as means ± standard deviations. Statistical analyses were performed using SPSS 11.0 (SPSS, Chicago, IL, USA). Statistical significance of the results was determined using Student's paired-samples t-test.

2.6. First-strand cDNA synthesis

Total RNAs extracted from samples were used for the synthesis of first-strand cDNAs by reverse transcriptase. Reverse transcription was performed in a final reaction volume of 9.5 µL containing 3 µg of the purified total RNA, 2 µL of 10 µM dT-ACP1 (5'-CTGTGAATGCTGCGACTACGATIIIIIT(18)-3'), and RNase-free water at 80 °C for 3 min. The mix was chilled on ice for 2 min, and 4 µL of 5X reaction buffer (Promega, USA), 5 µL of dNTPs (each 2 mM), 0.5 µL of RNasin RNase Inhibitor (40 U/µL; Promega), and 1 µL of Moloney murine leukemia virus reverse transcriptase (200 U/µL; Promega) were added. The final mix was incubated at 42 °C for 90 min and heated at 94 °C for 2 min. The tube was chilled on ice for 2 min and spun. First-strand cDNAs were diluted by the addition of 80 µL of ultrapurified water for the GeneFishing PCR and stored at –20 °C until use.

2.7. ACP-based GeneFishing PCR

Differentially expressed genes (DEGs) from control plants and and plants treated with 0.2 mM L^{-1} Ni were screened by the ACP-based PCR method (Kim et al., 2004) using GeneFishing DEG kits (Seegene, South Korea). Briefly, second-strand cDNA synthesis was conducted at 50 °C during 1 cycle of first-stage PCR in a final reaction volume of 20 µL containing 3–5 µL (about 50 ng) of diluted first-strand cDNA, 1 µL of dT-ACP2 (10 µM), 1 µL of 10 µM arbitrary ACP, and 10 µL of 2X Master Mix (Seegene). The PCR protocol for second-strand synthesis was 1 cycle at 94 °C for 5 min, followed by 50 °C for 3 min and 72 °C for 1 min. After second-strand DNA synthesis was completed, the second-stage PCR amplification protocol was 40 cycles of: 1) 94 °C for 40 s, 2) 65 °C for 40 s, and 3) 72 °C for 40 s, followed by 5 min of final extension at 72 °C. The amplified PCR products were separated on a 2% agarose gel stained with ethidium bromide.

2.8. Direct sequencing

The differentially expressed bands were reamplified and extracted from the gel using the GENCLEAN II Kit (Q-BIO gene, USA) and directly sequenced with an ABI PRISM 3100-*Avant* Genetic Analyzer (Applied Biosystems, USA) using a universal primer (5'-GTCTACCAGGCATTCGCTTCAT-3'). The sequences obtained were compared with the GenBank database using the BLAST network service (NCBI). All DEG experiments were done by Seegene.

3. Results

Alyssum corsicum seeds were grown in MS medium in the presence of 0.01 mM, 0.04 mM, and 0.2 mM nickel concentrations. After 2 months, multielement analysis was performed with harvested shoots and roots by PEDXRF. Total nickel concentration in shoots of *A. corsicum* increased in parallel with increasing nickel concentration in

media. The amount of nickel in shoots of *A. corsicum* plants reached 34.5 μg g^{-1}, 93.7 μg g^{-1}, and 932.5 μg g^{-1} with 0.01 mM, 0.04 mM, and 0.2 mM Ni concentrations, respectively. The amount of nickel in roots was 20.9 μg g^{-1}, 74.9 μg g^{-1}, and 499.7 μg g^{-1}. The results show that Ni is accumulated in the shoots more than in the roots (Figure 1). The results of PEDXRF multielement analysis show that the amounts of some other elements change with an increase in external Ni concentration. These selected elements are Mn, S, and Zn in shoots and Mg in roots (Figures 2A–2D). In shoots, the amounts of S (0.537%, 0.579%, 0.727%, 0.817%) and Zn (144.9, 126.9, 247.9, 268.1 μg/g) were increased with Ni concentrations (control, 0.01 mM, 0.04 mM, and 0.2 mM Ni concentration, respectively). The amount of Mn (0.035%, 0.036%, 0.040%, 0.044%, respectively) slightly increased. In the roots, however, the amount of S, Mn, and Zn did not correlate with increasing Ni concentrations; only magnesium slightly increased.

3.1. Trichomes and trichome density

SEM analysis of both the surfaces of leaves near the apical tips and lower parts of the stem was carried out in preliminary experiments. Analysis of the leaf surface with SEM showed that both the upper and lower epidermis of *A. corsicum* leaves was occupied by branched stellate trichomes. It was hard to see the epidermal cells and stoma through dense trichomes (Figures 3A and 3B). The upper sides of the trichome rays were covered with nodules on both surfaces (Figure 4). Although trichome density of both leaf surfaces was high in the control plants, it was gradually reduced with all nickel concentrations (Figures 5 and 6).

In addition, some changes in the trichome morphologies were also observed. The trichome centers lost their smooth surface, and some outgrowths were present at random places. Furthermore, the ray tips were slightly curved compared to those of the control plants at higher concentrations. As the nickel concentrations increased, some trichomes that had lost their dynamic structures were observed among the normal trichomes. They were of a puffed type and had reduced nodules (Figure 6). However, there was no significant difference with respect to metal concentration and metal contents between the 2 types of trichomes (data not shown).

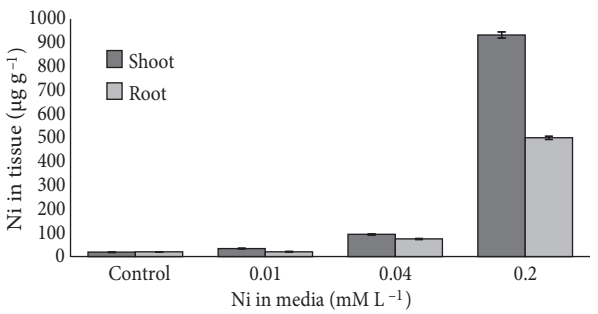

Figure 1. Nickel concentration in roots and shoots of *Alyssum corsicum* as a function of applied Ni concentration as determined by PEDXRF.

3.2. Distribution of Ni and other elements in leaves

EDX analysis of *Alyssum corsicum* leaves was carried out for the 4 metals, Ni, Mg, Ca, and Fe, in both control and Ni-treated specimens. The results are given as graphics in Figures 7A–7D. Nickel amount increased in all parts of the leaves (general surface, stoma, trichome centers, and trichome rays) in parallel with the 0.01 mM, 0.04 mM, and 0.2 mM nickel concentrations (Figure 7A). The stoma is the highest nickel-accumulating part on the upper surface. On the lower surface, the trichome rays accumulated the highest nickel concentrations. The stoma continued to accumulate nickel in parallel with the applied nickel concentration (data not shown). As we compared the 2 leaf surfaces with respect to the change in nickel concentrations, nickel accumulated more effectively at the stoma and trichome center on the upper surface. Nickel concentration increased more significantly in the trichome rays on the lower surface compared to those on the upper surface.

The concentrations of other elements varied with increasing nickel concentration. In all the examined parts of both leaf surfaces, nickel treatment decreased the amount of Mg compared with control conditions (Figure 7B). While the amount of Ca on the upper surfaces increased at the trichome center, rays, and stoma with 0.01 mM nickel concentration, it decreased significantly at 0.04 mM and 0.2 mM (Figure 7C). The amount of calcium on the lower surface was similar for both control and 0.01 mM Ni concentration treatments, whereas it decreased under higher concentrations. The amount of Fe decreased on both surfaces with increasing applied nickel concentrations (Figure 7D).

3.3. Protein analysis

The protein profiles of the plants with or without nickel exhibited 2 main bands of 49 kDa and 14 kDa in size respectively. They were identified as RuBisCo big and small subunits. There were no apparent differences in protein profiles between plants grown with nickel and without nickel.

3.4. Enzyme activities

CAT and GR activities in plants grown with nickel increased significantly as compared to plants grown without nickel at 0.01 mM Ni concentration. However, CAT and GR activity were decreased significantly ($P < 0.05$) in both shoots and roots after 0.04 and 0.2 mM nickel treatment. APX activity exhibited a significant increase only with 0.04 mM nickel treatment in both shoots and roots (Table 1).

3.5. DEGs

To investigate *Alyssum corsicum* responses to nickel, transcript levels in control and 0.2 mM Ni-treated

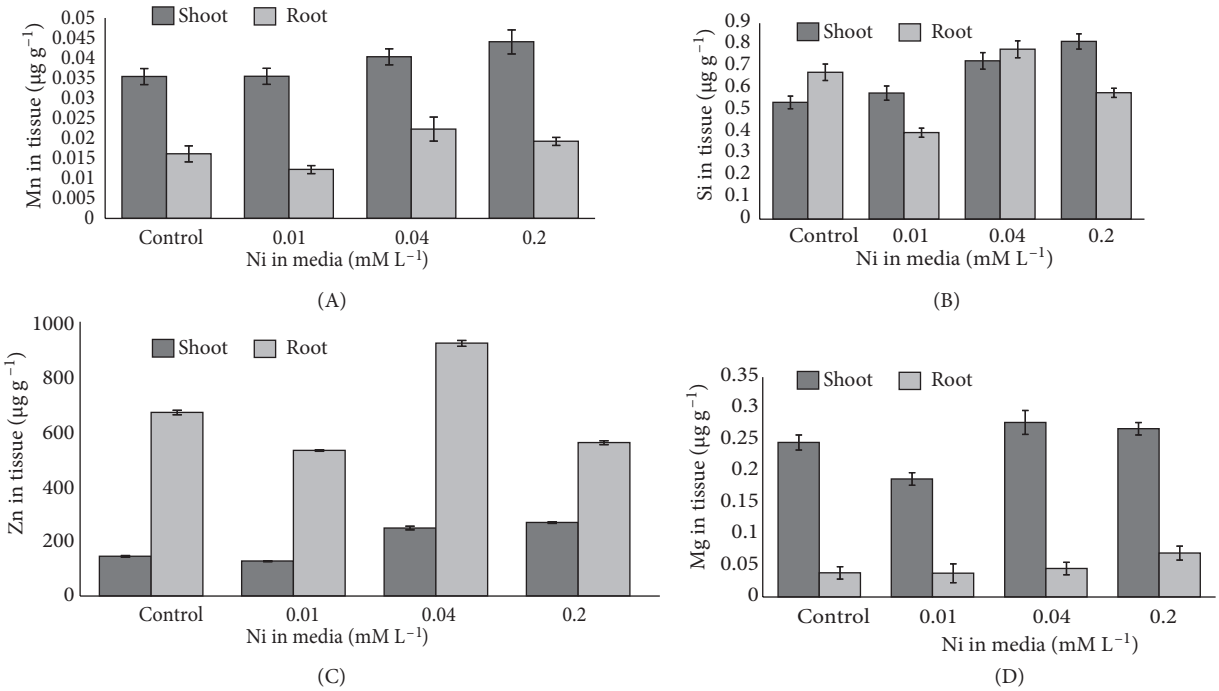

Figure. 2. Selected element concentrations in dry weight of *Alyssum corsicum* shoot and root parts as determined by PEDXRF after Ni treatment. A- Mn, B- S, C- Zn, D- Mg concentration.

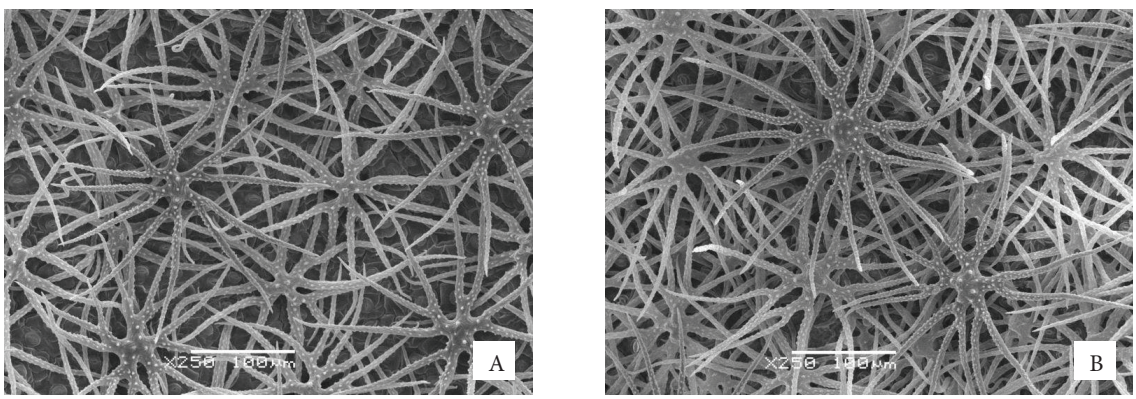

Figure 3. Upper and lower leaf surfaces of *Alyssum corsicum* control plant. A- Upper surface, B- lower surface.

plants were assessed by DEG primers. Different gene expression patterns were obtained in plants subjected to nickel treatment (Figure 8). Differential display patterns between nickel-treated and control plants showed that DEG1, DEG9, and DEG11 were overexpressed in control plants. They were 93% similar to *Arabidopsis thaliana* (L.) Heynh. first chromosome BAC T24P13, 60% similar to *Brassica rapa* L. subsp. *pekinensis* (Lour.) Kitam. clone KBrB081M20, and 99% similar to *Solms-laubachia eurycarpa* (Maxim.) Botsch.

DEG2, DEG3, DEG4, DEG5, DEG6, DEG7, DEG8, and DEG10 were overexpressed in plants grown with nickel. These DEGs were 68% similar to *Arabidopsis thaliana* calmodulin-binding protein (AT5G40190) mRNA, 72% similar to *Arabidopsis thaliana* hypothetical protein mRNA, 49% similar to *Arabidopsis thaliana* casein kinase II beta helix 3 (CKB3) mRNA, 99% similar to *Arabidopsis thaliana* Lhca2 protein (Lhca2) mRNA, 68% similar to *Arabidopsis thaliana* clone 30081 mRNA, 41% similar to *Arabidopsis thaliana* protease inhibitor/seed storage/lipid transfer protein (LTP) (AT4G22490) mRNA, 55% similar to *Brassica oleracea* L. var. *acephala* (DC.) Metzg. WSCP1R mRNA water-soluble chlorophyll protein, and 31% similar to *Arabidopsis thaliana* protease inhibitor/seed storage/LTP family (AT4G22490) mRNA (Table 2), respectively.

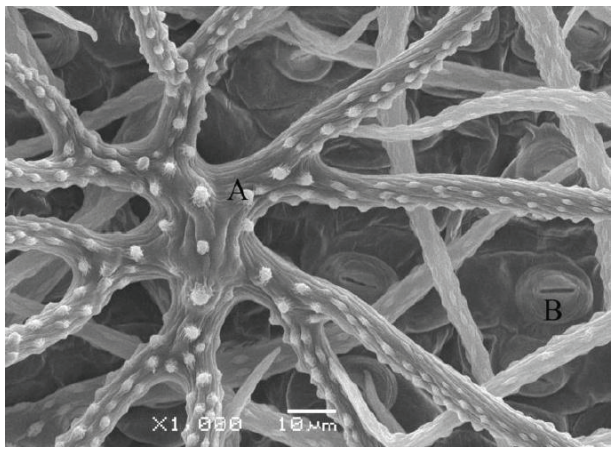

Figure 4. Nodules on the leaf trichome of *Alyssum corsicum*. A = Trichome, B = stoma.

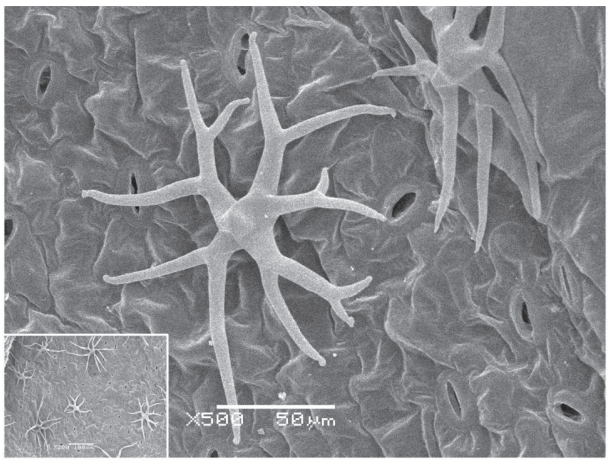

Figure 6. The differences observed in the leaf trichome structure and trichome density of *Alyssum corsicum* after treatment with 0.04 mM concentration of nickel (inset: at low magnification).

4. Discussion

Ni-hyperaccumulating *Alyssum* species such as *A. murale*, *A. bertolonii* Desv., *A. lesbiacum* (Cand.) Rech., and *A. corsicum* have been subject to many metal hyperaccumulation studies, both morphological and molecular (Krämer et al., 1997; Küpper et al., 2001; Kerkeb and Krämer, 2003; Bani et al., 2007). The data obtained will certainly address the storage status of the metals in plant tissues and be helpful for putting molecular studies in context.

This study is the first to examine the localization and distribution of nickel in *A. corsicum* grown under tissue culture conditions. Broadhurst et al. (2004) indicated that *A. murale* stored Ni primarily in the trichome pedicle, trichome basal compartment, and epidermal cells adjacent to the trichome attachment. The authors also stated that, at strongly phytotoxic Ni levels, the trichome density was greatly reduced with no overlapping trichomes. Krämer et al. (1997) also found that Ni was accumulated by epidermal trichomes on leaf surfaces of *Alyssum lesbiacum*. In our study, nickel was accumulated mainly in the stoma and the center of the trichomes on the upper surface; on the lower surface, Ni was accumulated slightly more in the trichome rays. Trichome density was reduced with increasing nickel concentrations. Psaras and Manetas (2001) opined that nickel is accumulated less in the seeds than in the vegetative parts of plants growing on metal-containing soils. Their results about the preferential accumulation of nickel in the cotyledon epidermis confirm the epidermal localization of nickel in the leaf tissues found in earlier studies. Our findings regarding the metal content of control plants show that the plants have a specific amount of nickel originating from the seed. McNear et al. (2005) remarked that metal accumulation in the trichome structure of *Alyssum murale* shows the functional role of trichomes in metal storage and detoxification although they are nonglandular. Psaras et al. (2000) proved the exclusion of nickel from guard cells of hyperaccumulator *Alyssum* species, and this led to the conclusion that the metal interferes with the normal stomatal function. However, to avoid the harmful effects of the metal, it is inactivated by the specific functions of the guard cells through the action of malate while migrating between the cytoplasm and the vacuole of the guard cells. In the research of Küpper et al. (2001), the amount of nickel in the large and elongated epidermal cells was more than that in the cells of the stomatal complexes; the authors indicated that this finding did not match with that of Heath et al. (1997), who reported that nickel was hyperaccumulated in the subsidiary cells within the stomatal complexes of the Ni-hyperaccumulator plant *Thlaspi montanum* L.

There are no previous reports about changes in the trichome structure in relation to nickel accumulation. In this study, we observed some changes in trichome

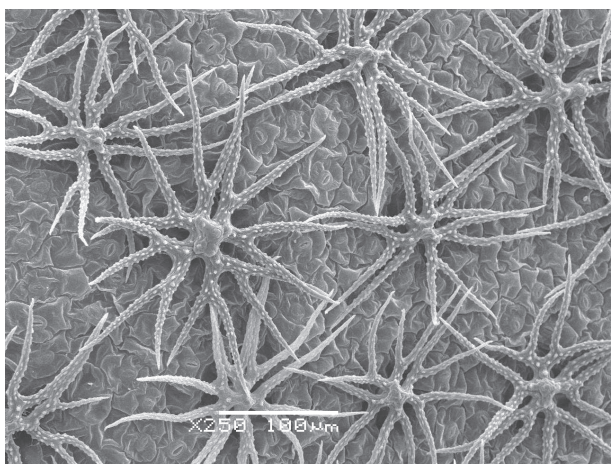

Figure 5. Upper leaf surface of *Alyssum corsicum* treated with 0.2 mM concentration of nickel.

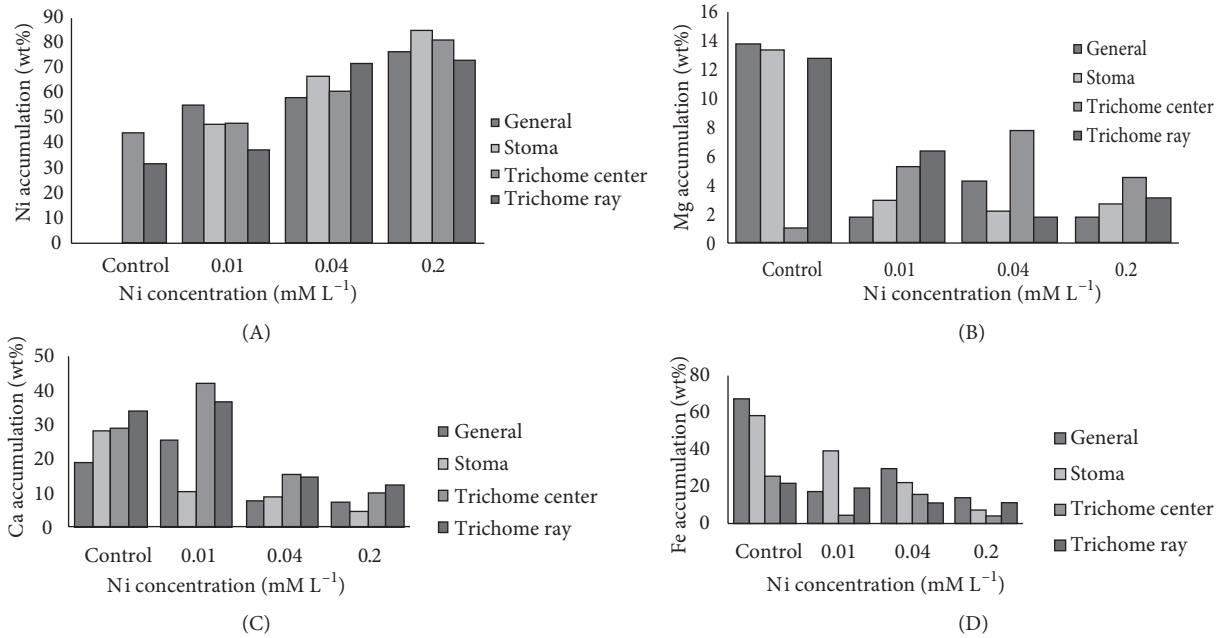

Figure 7. SEM-EDX analysis of some metals in the general upper surface of leaf, stoma guard cells, trichome center, and trichome rays of *Alyssum corsicum*. A- Ni, B- Mg, C- Ca, and D- Fe.

morphologies, such as presence of curves at ray tips and loss of surface smoothness in trichomes (Figure 6). One possible explanation is that high nickel accumulation may have changed some structural proteins in the trichomes, resulting in the loss of dynamic structure.

Some authors documented nodules on trichome surfaces (Psaras et al., 2000; Küpper et al., 2001; McNear et al., 2005), and these are suggested to contain calcium carbonate or oxalate crystallites (Broadhurst et al., 2004). Broadhurst et al. (2009) drew attention to a mechanism that enables trichome cells to push Ca and Mg into trichome rays while storing Ni and Mn in the base. Küpper et al. (1996) proposed that increased Mg levels may be a defense response of the plants to the substitution of Mg in chlorophyll by Ni or Cd. To some extent, our findings support these results. At an applied nickel concentration of 0.01 mM, Ca along with nickel is mostly accumulated in the trichome center and rays at both surfaces, but at 0.04 mM and 0.2 mM concentrations, the amount of Ca decreased in all of the parts. Robinson et al. (2003) indicated a competition between Ca and Ni uptake in plants, because increased Ni in the nutrient solution decreased the Ca concentrations in all parts of the plants. We observed similar results; at higher Ni concentrations, there was an inverse correlation between the accumulation of Ni and Ca. It seems that there is another competition between Mg and Ni for plant leaves because increasing levels of Ni in the medium caused the decrease of Mg in leaves of *A. corsicum*.

The PEDXRF results in this study show that the S amount in shoots is elevated in parallel with increasing nickel concentration (Figure 2B) The positive correlation of elevated Ni and S levels within epidermal cells has been reported by many authors (Krämer et al., 2000;

Table 1. GR, APX, and CAT enzyme activities in roots and shoots treated with nickel (µmol/min/mg protein).

Ni^{2+} concentration (mM L^{-1})	GR activity shoots	GR activity roots	APX activity shoots	APX activity roots	CAT activity shoots	CAT activity roots
Control	0.017 ± 0.0004	0.009 ± 0.0003	0.006 ± 0.0003	0.004 ± 0.0004	0.307 ± 0.0026	0.134 ± 0.0036
0.01	0.031 ± 0.0004*	0.011 ± 0.0004*	0.004 ± 0.0003*	0.004 ± 0.0002	0.522 ± 0.0062*	0.374 ± 0.0035*
0.04	0.026 ± 0.0003*	0.012 ± 0.0004*	0.008 ± 0.0005*	0.005 ± 0.0002*	0.310 ± 0.0046	0.308 ± 0.0036*
0.2	0.019 ± 0.0006*	0.007 ± 0.0004*	0.005 ± 0.0003	0.004 ± 0.0003	0.213 ± 0.005*	0.056 ± 0.0026*

Values represent averages ± standard deviations for triplicate measurements.
*: Significantly ($P < 0.05$) different from control.

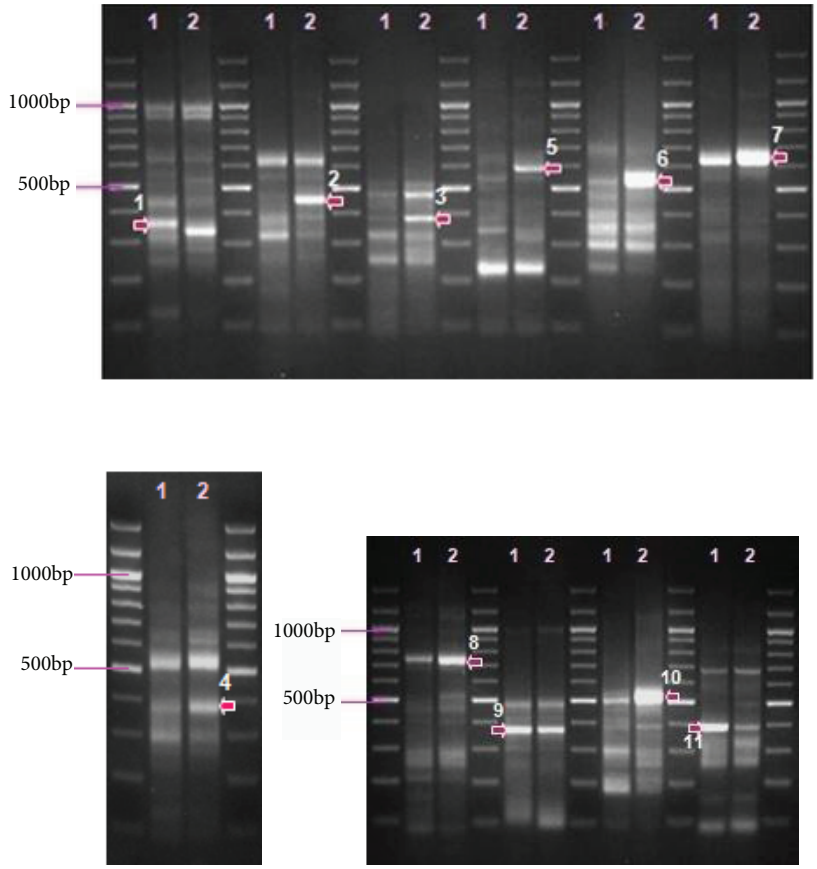

Figure 8. Differently expressed genes of control (1) and 0.2 mM L^{-1} nickel-treated *Alyssum corsicum* (2) with different DEGs primers (DEG1–DEG11; arrows).

Table 2. Overexpressed genes of *Alyssum corsicum* grown with nickel.

	Overexpressed DEG	Similarity search results
Control	DEG1	*Arabidopsis thaliana* (L.) Heynh. first chromosome BAC T24P13
	DEG9	*Brassica rapa* L. subsp. *pekinensis* (Lour.) Kitam. clone KBrB081M20
	DEG 11	*Solms-laubachia eurycarpa* maturase K (matK) gene gb|DQ409264.1| *Solms-laubachia eurycarpa* maturase K (matK) gene, partial cds; chloroplast length = 1765 Score = 509 bits (564), Expect = 2e-141 Identities = 304/317 (95%), Gaps = 1/317 (0%) Strand = Plus/Plus
0.2 mM L^{-1} nickel-treated plant	DEG2	*Arabidopsis thaliana* calmodulin-binding protein (AT5G40190) mRNA
	DEG3	*Arabidopsis thaliana* hypothetical protein mRNA
	DEG4	*Arabidopsis thaliana* CKB3 (casein kinase II beta helix 3) mRNA
	DEG5	*Arabidopsis thaliana* Lhca2 mRNA (Lhca2)
	DEG6	*Arabidopsis thaliana* clone 30081 mRNA
	DEG7	*Arabidopsis thaliana* protease inhibitor/seed storage/lipid transfer proteins (LTP) (AT4G22490) mRNA
	DEG8	*Brassica oleracea* var. *acephala* WSCP1R mRNA water-soluble chlorophyll protein
	DEG10	*Arabidopsis thaliana* protease inhibitor/seed storage/lipid transfer protein (LTP) family (AT4G22490) mRNA

Küpper et al., 2001; Broadhurst et al., 2004). We observed similar correlations between Ni and the metals Mn and Zn in shoots of *A. corsicum* (Figures 2A and 2C) at higher concentrations. Tappero et al. (2007) showed that Mn amounts increased in parallel with an increase in nickel concentrations. Broadhurst et al. (2004, 2009) observed that Ni and Mn were co-located and strongly concentrated only in the trichome base and in the cells adjacent to trichomes. Broadhurst et al. (2004) also found that Mn and Zn levels were elevated in *Alyssum* species across a series of Ni additions as compared to control plants.

Protein banding profiles determined by SDS-PAGE were not different for control and nickel-treated plants. However, other techniques would likely be more successful in determining the differences at the protein level, such as 2D gel electrophoresis or MALDI-TOF/MS. In this work, however, we observed differences in antioxidant enzyme activity in roots and shoots of *A. corsicum* plant upon nickel treatment (Table 1). We observed enhanced CAT and GR activity in plants grown with lower nickel concentrations. In the case of APX, activity exhibited an increase only with 0.04 mM nickel treatment in both shoots and roots ($P < 0.05$). CAT is one of the key enzymes in the removal of toxic peroxides. An increase in the activity of CAT has been reported in certain plant species exposed to toxic concentrations of heavy metals such as Cu, Pb, and Zn. Decline in CAT activity is regarded as a general response to many stresses, and it is supposedly due to inhibition of enzyme synthesis or a change in assembly of enzyme submits (Shah et al., 2001). Low levels of Ni^{2+} induced GR activity significantly in shoots and slightly in roots. However, this activity was reduced at higher Ni^{2+} concentrations. The increase in the activity of GR upon heavy metal treatment may result from the fact that the glutathione/ascorbate cycle is operating at a high rate in order to detoxify the ROS formed as a result of heavy metal treatment or that glutathione has to be recycled back into the reduced form before its incorporation into phytochelatins (metallothionein-like proteins) (Fatima and Ahmad, 2004). The decrease in GR activity at high concentrations may also be the result of the metal's direct reaction with sulfhydryl groups interfering with the glutathione cycle. APX activity may have been compensated for by the activation of other isoperoxidases that were not detected by the assay (Schickler and Caspi, 1999).

Genes responding to changes in nickel exposure in *A. corsicum* were identified using DEG primers. Eleven different DEGs were identified whose expression patterns were altered under nickel stress (Table 2). Among the 11 genes most differently expressed between nickel deficiency and sufficiency exposures were the BAC T24P13 part genomic sequence, Lhca2 protein (Lhca2) mRNA sequence, *Solms-laubachia eurycarpa* maturase K (matK) gene, calmodulin-binding protein (AT5G40190), hypothetical protein mRNA, CKB3, Lhca2 protein (Lhca2), and protease inhibitor/seed storage/LTP. One of the genes overexpressed upon exposure of *A. corsicum* to nickel deficiency was matK (sequence similar to *Solms-laubachia eurycarpa* (Maxim.) Botsch.), along with the Lhca2 code for the light harvesting protein. Casein kinase II beta helix served as ribosome biogenesis.

Metal hyperaccumulator plants have been subject to many studies in recent years with the collaboration of different disciplines. The potential advantage of plant species in a remediation technique that is low-cost and harmless to human health and the environment will be a valuable addition to existing methods of remediation. Understanding the mechanism underlying the metal accumulation ability would facilitate not only phytoremediation studies but also plant physiology studies concerning the heavy metal metabolism of plants.

Acknowledgments

We would like to thank the State Planning Organization for providing funding for the 2003K120470/02-coded project including this study and for financial support for this research (Grant No. 1998K121480).

References

Abou Auda MM, Symeonidis L, Hatzistavrou E, Yupanis T (2002). Nucleolytic activities and appearance of a new DNase in relation to nickel and manganese accumulation in *Alyssum murale*. J Plant Physiol 159: 1087–1095.

Altınözlü H, Karagöz A, Polat T, Ünver İ (2012). Nickel hyperaccumulation by natural plants in Turkish serpentine soils. Turk J Bot 36: 269–280.

Bani A, Echevarria G, Sulçe S, Morel JL, Mullai A (2007). In-situ phytoextraction of Ni by a native population of *Alyssum murale* on an ultramafic site (Albania). Plant Soil 293: 79–89.

Boominathan R, Doran PM (2002). Ni-induced oxidative stress in roots of the Ni hyperaccumulator, *Alyssum bertolonii*. New Phytol 156: 205–215.

Bradford MM (1976). Rapid and sensitive method for the quantitation of microgram quantities of protein utilizing the principle of protein-dye binding. Anal Biochem 72: 248–254.

Broadhurst CL, Chaney J, Angle JS, Erbe EF, Maugel TK (2004). Nickel localization and response to increasing Ni soil levels in leaves of the nickel hyperaccumulator *Alyssum murale*. Plant Soil 265: 225–242.

Broadhurst CL, Tappero RV, Maugel TK, Erbe EF, Sparks DL, Chaney RL (2009). Interaction of nickel and manganese in accumulation and localization in leaves of the Ni hyperaccumulators *Alyssum murale* and *Alyssum corsicum*. Plant Soil 314: 35–48.

Brooks RR (2000). Phytoarchaelogy and hyperaccumulators. In: Brooks RR, editor. Plants that Hyperaccumulate Heavy Metals: Their Role in Phytoremediation, Microbiology, Archaeology, Mineral Exploration and Phytomining. Cambridge: CAB International, pp. 153–180.

Çakmak I (1994). Activity as ascorbate-dependent H_2O_2 scavenging enzymes and leaf chlorosis are enhanced in magnesium- and potassium-deficient leaves but not in phosphorus-deficient leaves. J Ex Bot 45: 1259–1266.

Clemens S (2001). Molecular mechanisms of plant metal tolerance and homeostasis. Planta 212: 475–486.

Fatima RA, Ahmad M (2004). Certain antioxidant enzymes of *Allium cepa* as biomarkers for the detection of toxic heavy metals in wastewater. Sci Total Environ 346: 256–273.

Guo TR, Zhang GP, Zhang YH (2007). Physiological changes in barley plants under combined toxicity of aluminum, copper and cadmium. Colloids Surf B 15: 182–188.

Hajduch M, Rakwal R, Agrawal R, Yonekura M, Pretova A (2001). High resolution two-dimensional electrophoresis separation of proteins from metal stressed rice (*Oryza sativa* L.) leaves. Electrophoresis 22: 2824–2831.

Heath SM, Southworth D, D'Allura JA (1997). Localization of nickel in epidermal subsidiary cells of leaves of *Thlaspi montanum* var. *Siskiyouense* (Brassicacea) using energy dispersive x-ray microanalysis. Int J Plant Sci 158: 184–188.

Johnson DM, Hooper PR, Conrey RM (1999). XRF Analysis of Rocks and Minerals for Major and Trace Elements on a Single Low Dilution Li-tetraborate Fused Bead. Newtown Square, PA, USA: International Centre for Diffraction Data.

Kerkeb L, Krämer U (2003). The role of free histidine in xylem loading of nickel in *Alyssum lesbiacum* and *Brassica juncea*. Plant Physiol 131: 716–724.

Krämer U, Charnack JM, Baker AJM (1996). Free histidine as a metal chelator in plants that accumulate nickel. Nature 379: 635–638.

Krämer U, Grime GW, Smith JAC, Hawes CR, Baker AJM (1997). Micro-PIXE as a technique for studying nickel localization in leaves of the hyperacccumulator plant *Alyssum lesbiacum*. Nucl Instrum Methods 130: 346–350.

Krämer U, Pickering IJ, Prince RC, Raskin I, Salt DE (2000). Subcellular localization and speciation of nickel in hyperaccumulator and non-hyperaccumulator *Thlaspi* species. Plant Physiol 122: 1343–1353.

Küpper H, Küpper F, Spiller M (1996). Environmental relevance of heavy metal- substituted chlorophylls using the example of water plants. J Ex Bot 47: 259–266.

Küpper H, Lombi E, Zhao FJ, Wieshammer G, McGrath SP (2001). Cellular compartmentation of nickel in the hyperaccumulators *Alyssum lesbiacum*, *Alyssum bertolonii* and *Thlaspi goesingense*. J Ex Bot 52: 2291–2300.

Laemli UK (1970). Cleavage of structural proteins during the assembly of the head of the bacteriophage T4. Nature 277: 680–684.

Margui E, Queralt I, Carvalho ML, Hidalgo M (2005). Comparison of EDXRF and ICP349 after microwave digestion for element determination in plant specimens from an abandoned mining area. Anal Chim Acta 549: 197–204.

Marmiroli M, Gonnelli C, Maestr E, Gabbriell R, Marmiroli N (2004). Localisation of nickel and mineral nutrients Ca, K, Fe, Mg by scanning electron microscopy microanalysis in tissues of the nickel-hyperaccumulator *Alyssum bertolonii* Desv. and the non-accumulator *Alyssum montanum*. Plant Biosystems 138: 231–243.

McNear DH, Peltier E, Everhart J, Chaney RL, Sutton S, Newville M, Rivers M, Sparks DL (2005). Application of quantitative fluorescence and absorption-edge computed microtomography to image metal compartmentalization in *Alyssum murale*. Environ Sci Technol 39: 2210–2218.

Murashige T, Skoog F (1962). A revised medium for rapid growth and bioassays with tobacco tissue culture. Plant Physiol 15: 473–497.

Öztürk Ürek R, Tarhan L (2012). The relationship between the antioxidant system and phycocyanin production in *Spirulina maxima* with respect to nitrate concentration. Turk J Bot 36: 369–377.

Pilon-Smits E (2005). Phytoremediation. Annu Rev Plant Biol 56: 15–39.

Prasad MNV (2005). Nickelophilous plants and their significance in phytotechnologies. Braz J Plant Physiol 17: 113–128.

Psaras GK, Constantinidis TH, Cotsopoulos B (2000). Relative abundance of nickel in the leaf epidermis of eight hyperaccumulators: evidence that the metal is excluded from both guard cells and trichomes. Ann Bot 86: 73–78.

Psaras GK, Manetas Y (2001). Nickel localization in seeds of the metal hyperaccumulator *Thlaspi pindicum* Hausskn. Ann Bot 88: 513–516.

Reeves RD, Adıgüzel N (2008). The nickel hyperaccumulating plants of the serpentines of Turkey and adjacent areas: a review with new data. Turk J Biol 32: 143–153.

Robinson BH, Lombi E, Zhao FJ, McGrath SP (2003). Uptake and distribution of nickel and other metals in the hyperaccumulator *Berkheya coddii*. New Phytol 158: 279–285.

Schickler H, Caspi H (1999). Response of antioxidative enzymes to nickel and cadmium stress in hyperaccumulator plants of the genus *Alyssum*. Phyisol Plant 105: 39–44.

Shah K, Kumar RG, Verma S, Dubey RS (2001). Effect of cadmium on lipid peroxidation, superoxide anion generation and activities of antioxidant enzymes in growing rice seedlings. Plant Sci 161: 1135–1144.

Tappero R, Peltier E, Gräfe M (2007). Hyperaccumulator *Alyssum murale* relies on a different metal storage mechanism for cobalt than for nickel. New Phytol 17: 641–654.

Timothy E, Tour L (1989). Analysis of rocks using X-ray fluorescence spectrometry. Rigaku Journal 6: 3–9.